

Black holes with non-Abelian hair and their thermodynamical properties

Takashi Torii and Kei-ichi Maeda*

Department of Physics, Waseda University, Shinjuku-ku, Tokyo 169-50, Japan

(Received 8 March 1993)

We present some black-hole solutions of the Einstein-Yang-Mills-dilaton system and calculate their Hawking temperatures. We find that if the coupling constant of the dilaton is smaller than some critical value, the thermodynamical behavior of these black holes includes two phase transitions at points determined by the value of the mass parameter. The black holes with masses between those two critical values have a positive specific heat. This is also true for the known colored black-hole solutions. We also reanalyze Skyrme black holes and find that there exist two types of solutions (a stable type and an unstable excited type) and these two types converge to a bifurcation point at some critical horizon radius, beyond which there is no Skyrme black hole. The stable black holes have two possible fates: they can evaporate via the Hawking process, and so evolve into a particlelike (Skyrmion) solution, or they can accrete matter and evolve into the Schwarzschild solution. When a Skyrme black hole evolves into a Schwarzschild black hole, its area changes discontinuously, so that we may regard this evolution as a kind of first-order phase transition. The specific heat of stable Skyrme black holes is always negative, while there are either one or three transition points for unstable Skyrme black holes.

PACS number(s): 04.20.Jb, 04.50.+h, 11.15.-q, 97.60.Lf

I. INTRODUCTION

The exterior gravitational field of a stationary source may have infinitely many independent multipole moments. But when that source lies within an event horizon, a radical simplification occurs: all its multipole moments are then uniquely determined by two parameters M and a , interpretable physically as the mass and angular momentum of the source. When the source has a net charge Q , then of course that parameter is also required to uniquely determine its (electric and gravitational) multipole moments. But a series of theorems culminating in the work of Mazur [1] show that no other parameters are required to determine a stationary black-hole solution in Einstein-Maxwell theory. As Wheeler puts it, "a black hole has no hair."

The work of Bekenstein [2], Hartle [3], and Teitelboim [4] shows that stationary black-hole solutions are similarly hairless in a variety of theories coupling classical fields to Einstein gravity, so the recent discovery of a particlelike solution [5] and a colored black-hole solution [6] in the Einstein-Yang-Mills (EYM) theory came as quite a surprise. It is true, of course, that recent work has shown these solutions are unstable [7]. But if this instability deprives them of physical meaning, it does not diminish their interest as counterexamples to one non-Abelian generalization of the above no hair theorem. Further, this instability seems to be inessential. The black-hole solutions of the Einstein-Skyrme (ES) theory also have

non-Abelian hair [8,9], and are known to be stable under linear perturbations [10].

In this paper, first we study static black holes in a theory that couples a scalar field to a Yang-Mills (YM) field. The theory we consider arises as the four-dimensional effective theory corresponding to various higher-dimensional unified theories of fundamental interactions, and the scalar field it contains, which we shall call the dilaton field, is an artifact of the scale invariance typical of these unified theories. Our goal is to determine how this dilaton field affects the structure and thermodynamics of non-Abelian black holes. We present numerical solutions representing dilatonic colored black holes in the Einstein-Yang-Mills-dilaton (EYMD) system [11] and we discuss the effect of the dilaton coupling on their structure (Sec. II). We also calculate their Hawking temperatures and examine their thermodynamical properties (Sec. III).

Several years ago, in a simpler gravitational system, the Einstein-Maxwell-dilaton (EMD) system, a black-hole solution and its thermal properties were discussed by Gibbons and one of the present authors [12]. It was shown that a second-order phase transition (change in sign of the specific heat), which also appears in the case of a Reissner-Nordström black hole, does not occur when the coupling constant of the dilaton α is greater than unity. From our numerical analysis, we find that a dilatonic colored black hole has similar phase transitions at two points, if α is smaller than a critical coupling constant $\alpha_{cr} \sim 0.5$ (Sec. III).

We also reanalyze the black-hole solutions of the ES system and calculate their Hawking temperatures. It turns out that the ES system has two types of black-hole solutions [8]: one is the stable type discussed in

*Electronic address: maeda@jpnwas00.bitnet or maeda@cfi.waseda.ac.jp

Ref. [10] and the other is an excited type which is unstable [13]. These two types converge to a bifurcation point when each has the same critical horizon radius, and beyond this point there is no solution except for the Schwarzschild solution. This fact suggests a scenario for their evolution which we will discuss below (Sec. IV). No phase transition occurs for the stable type, while the excited type has either one or three phase transition points as in the EYM or EYMD system (Sec. V).

II. DILATONIC COLORED BLACK HOLES

We consider models with the action [14],

$$S = \int d^4x \sqrt{-g} \left[\frac{1}{2\kappa^2} R(g) - \frac{1}{2\kappa^2} (\nabla\Phi)^2 - \frac{1}{16\pi g_C^2} e^{-\alpha\Phi} \text{Tr} F^2 \right], \quad (1)$$

where $\kappa^2 = 8\pi G$, Φ is the dilaton field, and F and A are the YM field strength and its potential, respectively, i.e., $F = dA + A \wedge A$. g_C and $\alpha (\geq 0)$ are coupling constants for the YM field and the dilaton field, respectively. This type of action arises from various unified theories

including a superstring model; for details, see [12]. For example, $\alpha = 1$ and $\alpha = \sqrt{3}$ are the cases arising from superstring theory and from the five-dimensional Kaluza-Klein theory, respectively. Notice that $\alpha = 0$ with $\Phi = 0$ denotes the usual EYM system.

We now consider an SU(2)-YM field, although this is inessential: we can easily extend our analysis to any gauge group that has an SU(2) subgroup [15]. We shall assume a spherically symmetric ansatz. In the spherically symmetric static case the space-time metric can be written as

$$ds^2 = - \left(1 - \frac{2Gm}{r} \right) e^{-2\delta} dt^2 + \left(1 - \frac{2Gm}{r} \right)^{-1} dr^2 + r^2 (d\theta^2 + \sin^2\theta d\phi^2). \quad (2)$$

For the YM potential, we consider only the purely “magnetic” case, i.e.,

$$A = w\tau_1 d\theta + (\cos\theta\tau_3 + w\sin\theta\tau_2) d\phi, \quad (3)$$

where τ_i denote the generators of SU(2). m , δ (the metric), and w (the YM potential) are functions only of the radial coordinate r .

Variation of the action (1) leads to the field equations

$$\bar{m}' = \frac{\bar{r}^2}{4} \left(1 - \frac{2\bar{m}}{\bar{r}} \right) \Phi'^2 + \frac{1}{\lambda_H^2} e^{-\alpha\Phi} \left\{ \left(1 - \frac{2\bar{m}}{\bar{r}} \right) w'^2 + \frac{1}{2\bar{r}^2} (1 - w^2)^2 \right\}, \quad (4)$$

$$\delta' = -\frac{\bar{r}}{2} \Phi'^2 - \frac{2}{\lambda_H^2} \frac{e^{-\alpha\Phi}}{\bar{r}} w'^2, \quad (5)$$

$$\left[e^{-\delta\bar{r}^2} \left(1 - \frac{2\bar{m}}{\bar{r}} \right) \Phi' \right]' + \frac{2}{\lambda_H^2} \alpha e^{-(\delta+\alpha\Phi)} \left[\left(1 - \frac{2\bar{m}}{\bar{r}} \right) w'^2 + \frac{1}{2\bar{r}^2} (1 - w^2)^2 \right] = 0, \quad (6)$$

$$\left[e^{-(\delta+\alpha\Phi)} \left(1 - \frac{2\bar{m}}{\bar{r}} \right) w' \right]' + e^{-(\delta+\alpha\Phi)} \frac{1}{\bar{r}^2} w (1 - w^2) = 0, \quad (7)$$

where we have introduced the dimensionless variables \bar{r} and \bar{m} , normalized by the radius of the horizon r_H , i.e., $\bar{r} = r/r_H$ and $\bar{m} = Gm/r_H$. A prime denotes a derivative with respect to \bar{r} . $\lambda_H \equiv r_H/[l_P/g_C]$, where $l_P \equiv \sqrt{G}$ is the Planck length, denotes the ratio of the size of black hole to a typical scale length of the present theory ($\sim l_P/g_C$). The above expression of the basic equations has the advantage that it includes only one dimensionless free parameter λ_H . All black holes with the same value of λ_H are described by the same solution. When we wish to consider a large black hole, we have only to take the limit $\lambda_H \rightarrow \infty$. In this limit, we recover the spherically symmetric Einstein equations with a massless scalar field. The solution with a regular horizon is just the Schwarzschild black hole.

In order to find a black-hole solution of Eqs. (4)–(7), we have to discuss in advance the boundary conditions on the event horizon and at infinity. First we assume a regular event horizon at $\bar{r} = 1$, i.e.,

$$\bar{m}_H = \frac{1}{2}, \quad |\delta_H| < \infty, \quad (8)$$

where the subscript H denotes evaluation of functions at the horizon. Outside the horizon, the condition $r > 2m(r)$ must be satisfied. From Eqs. (6) and (7) we find the following relations on the horizon, which determine the functions Φ and w for $r \geq r_H$:

$$\Phi'_H = -\frac{\alpha e^{-\alpha\Phi_H} (1 - w_H^2)^2}{\lambda_H^2 \left[1 - \lambda_H^{-2} e^{-\alpha\Phi_H} (1 - w_H^2)^2 \right]}, \quad (9)$$

$$w'_H = -\frac{(1 - w_H^2) w_H}{1 - \lambda_H^{-2} e^{-\alpha\Phi_H} (1 - w_H^2)^2}. \quad (10)$$

To find asymptotically flat solutions, we must have

$$m(r) \rightarrow M = \text{const}, \quad \delta(r) \rightarrow \delta_\infty = 0 \quad \text{as } r \rightarrow \infty, \quad (11)$$

where M is the gravitational mass of our sought-for black hole. As for Φ and w , we assume $\Phi \rightarrow 0$ and $w \rightarrow \pm 1$ as $r \rightarrow \infty$, which guarantees the finiteness of the energy of the system.

Because we have to impose six boundary conditions [Eqs. (9) and (10), and $|w| = 1, w' = \Phi = \Phi' = 0$ at infinity] on two second-order differential equations (6) and (7), we have too many boundary conditions to obtain a solution with arbitrary values of Φ_H and w_H . Rather we have to solve those basic equations as an eigenvalue problem. When we solve the above Eqs. (6) and (7) iteratively; therefore, we first guess the values of two free shooting parameters Φ_H and w_H and integrate the equations numerically until we find a solution consistent with all boundary conditions. We can assume $w_H > 0$ without loss of generality, since we can obtain solutions with $w_H < 0$ from those by a gauge transformation.

Under the above conditions, we solved Eqs. (4)–(7) numerically and found a discrete family of regular black-hole solutions characterized by the node number (n) of the YM potential. For $\lambda_H = 1$, the solutions with one node ($n = 1$) for various values of α are shown in Fig. 1. We can see that the dilaton field Φ increases as the

coupling constant α increases. But as α increases further, Φ decreases again. This is to be expected, because in the limit of $\alpha \rightarrow \infty$, we must recover a Schwarzschild solution ($\bar{m} = \frac{1}{2}$ and $\delta = 0$) with $\Phi = 0$. The YM field also vanishes, ($w = 1$) for the same reason. We confirmed these behaviors in our numerical calculation, although we have not shown them in our figures. For the solution with $n = 2$ (two nodes) the YM field extends a larger distance. (See the dashed line in the figure.)

In Fig. 2, we also show solutions for various values of λ_H , setting $\alpha = 1$. When $\lambda_H \rightarrow \infty$, i.e., $r_H \rightarrow \infty$ (large black holes) or $g_C \rightarrow \infty$, we find that the space-time approaches the Schwarzschild solution, while the YM potential w is not trivial ($w \neq 1$). This is easy to understand, because in the limit $\lambda_H \rightarrow \infty$, the YM field decouples from gravity [see Eqs. (4)–(7)]. The non-Abelian YM field can then have a nontrivial configuration although it makes no contribution to the black-hole structure (see Fig. 2).

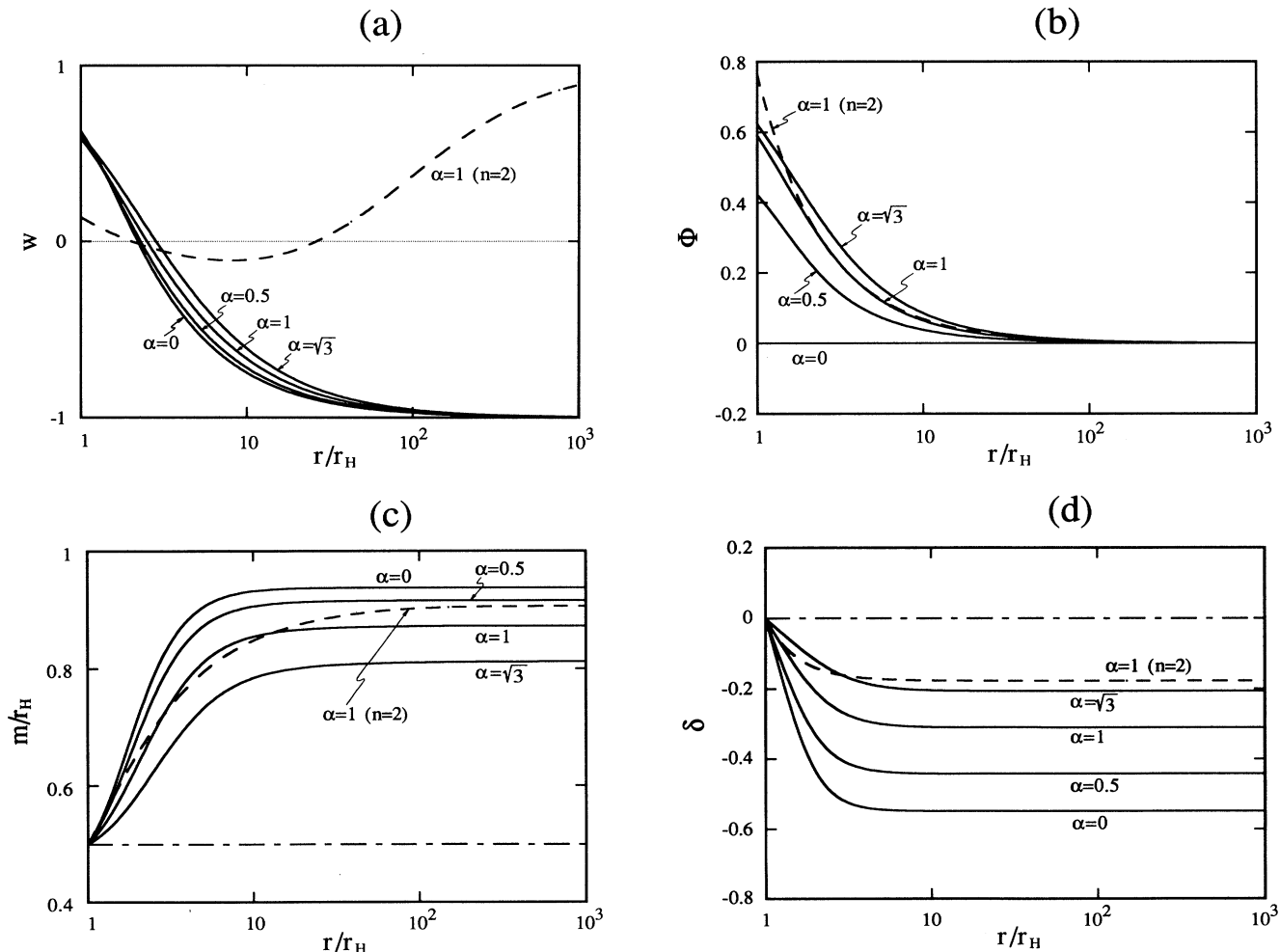


FIG. 1. The solutions of (a) the Yang-Mills potential w , (b) the dilaton field Φ , (c) the mass function m , and (d) the lapse function δ for dilaton colored black holes with one node ($n = 1$). We set $\lambda_H = 1$ and show the models for $\alpha = 0, 0.5, 1, \sqrt{3}$. The solution for $\alpha = 0$ corresponds to the colored black hole. $\alpha = 1$ and $\alpha = \sqrt{3}$ are the models from superstring theory and from the five-dimensional Kaluza-Klein theory, respectively (see Ref. [12]). We also show the $n = 2$ model of $\alpha = 1$ (dashed line). In the limit of $\alpha \rightarrow \infty$, the solution approaches the Schwarzschild solution [the dot-dashed line in (c) and (d)].

What physically happens when the black hole gets large is as follows. For each node number n , a particlelike solution has a unique mass and charge, which are a dimensionless factor of order unity times m_P/g_C and $1/g_C$, respectively. When we put a black hole at the center of such a solution, the black hole swallows a part of the YM field and leaves the rest outside its horizon as a “cloud.” In order to discuss such a structure when the black hole gets large, we introduce an effective charge for the black hole, $Q_{\text{eff}} \equiv e^{-\alpha\Phi_H}(1 - w_H^2)/g_C$, which results from performing a surface integration of the YM field at the horizon, just as does the electric charge in Maxwell theory.

The typical scale of the “particle” is l_P/g_C . Hence, if the size of the black hole is smaller than this value, only a part of the “particle” lies within the black hole. As the black hole gets larger, it swallows more and more of the ambient YM field, so that its effective charge increases with respect to its horizon radius, as shown in Fig. 3. Since the “particle” appears neutral to an observer at

infinity, we might expect that its effective charge would tend to zero when the black hole gets larger than the scale of the “particle.” However, this expectation is mistaken. As we can see from Fig. 3, the effective charge of the black hole converges to some finite value after its size becomes larger than that of the “particle.” The black hole does not swallow the whole structure of the YM field. When the black hole gets large, however, the energy of the YM field outside of the black hole, defined by

$$E_{\text{YM}}(r_H) \equiv - \int_{r_H}^{\infty} T_0^0 \sqrt{-g} d^3x, \quad (12)$$

has the asymptotic behavior $E_{\text{YM}}(r_H) \sim Q_{\text{eff}}^2/r_H$, which vanishes in the limit $r_H \rightarrow \infty$ (see Fig. 4). The effect of the YM field energy density on the space-time structure becomes smaller when the black hole is larger, so that a Schwarzschild black hole results in the limit $r_H \rightarrow \infty$, as we have explained earlier. However, because the black hole does not swallow the whole structure of the “parti-

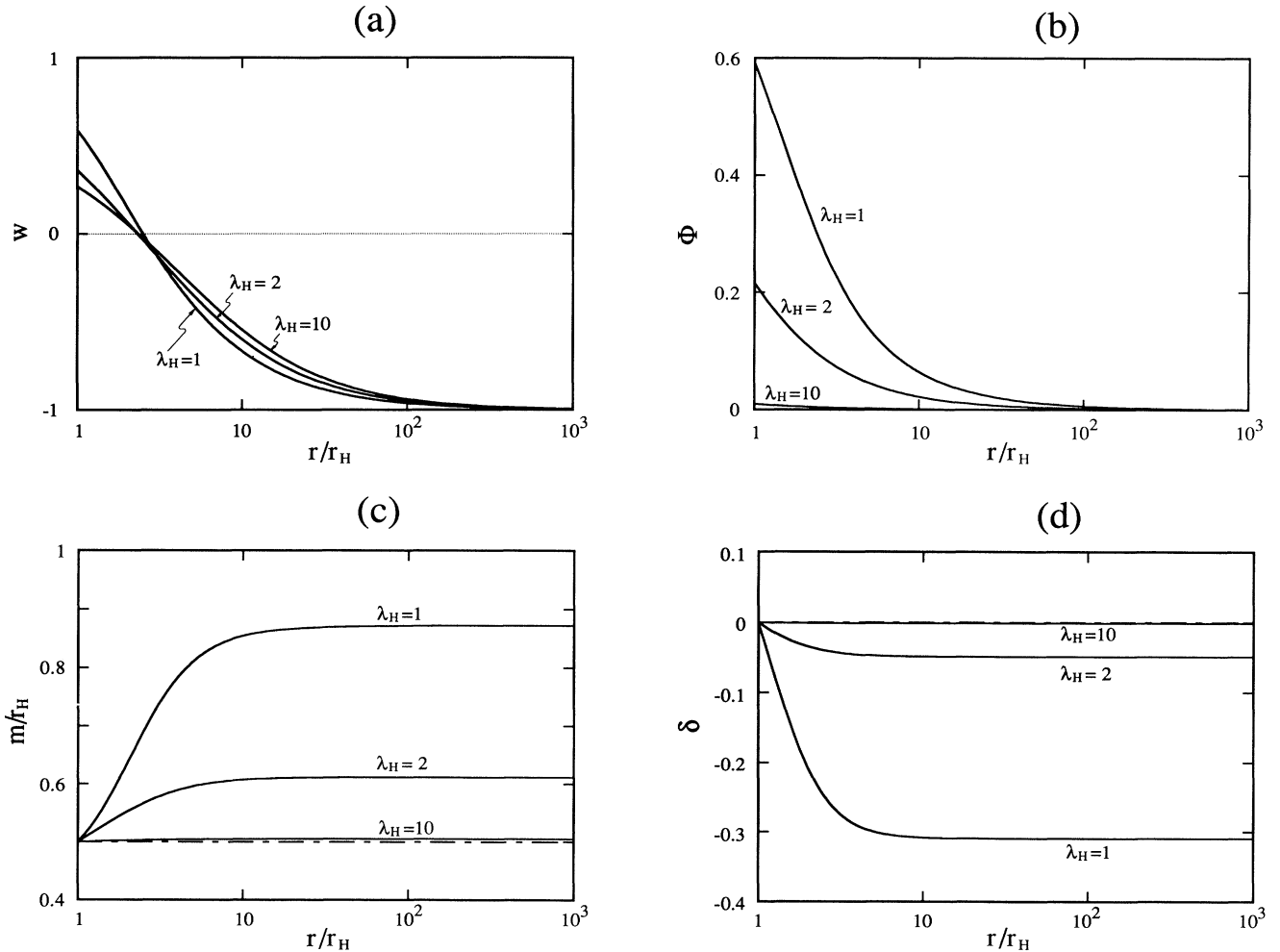


FIG. 2. The solutions of (a) the Yang-Mills potential w , (b) the dilaton field Φ , (c) the mass function m , and (d) the lapse function δ for dilaton colored black holes with one node ($n = 1$). We set $\alpha = 1$ and show the models for $\lambda_H = 1, 2, 10$. We also plot the Schwarzschild solution by a dot-dashed line for comparison. In the limit of $\lambda_H \rightarrow \infty$, we find the Schwarzschild black hole with nontrivial non-Abelian structure.

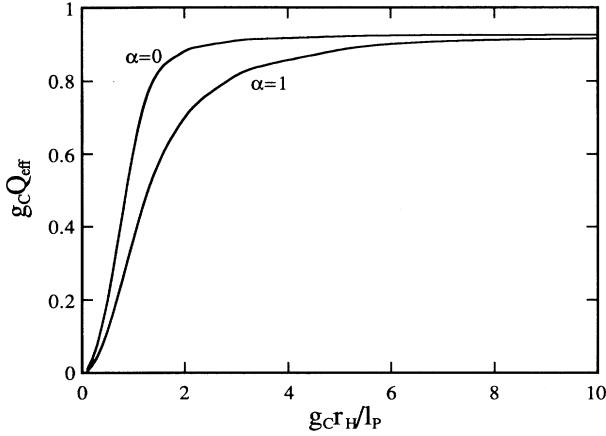


FIG. 3. The effective YM charge Q_{eff} of the colored black hole. Below the scale of a particlelike solution ($\sim l_P/g_C$), Q_{eff} increases with respect to λ_H . However, beyond that scale, Q_{eff} converges to a finite value.

cle,” and the black-hole charge tends to a nonzero limit, the YM field energy outside the horizon turns out to be much larger than the energy of the original “particle” (i.e., the YM field energy of the particlelike solution integrated from r_H to infinity; see Fig. 4).

We conclude that when the black hole gets large, it acquires a definite charge, which is fixed by m_P , g_C , and a node number n . This charge constitutes a sort of non-Abelian hair.

III. THERMODYNAMICAL PROPERTIES OF DILATONIC COLORED BLACK HOLES

The black holes considered here may be rather small unless $g_C \ll 1$, because their typical size is probably

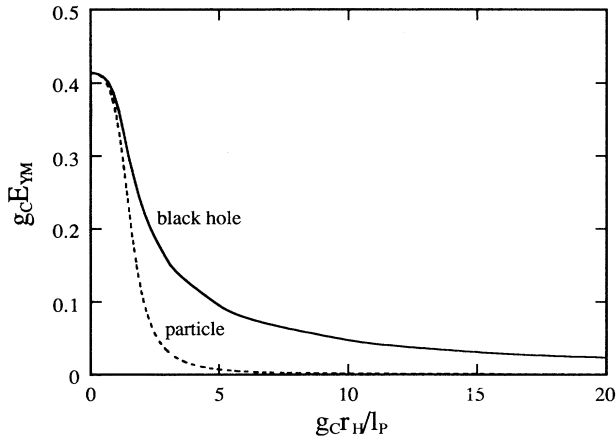


FIG. 4. The energy of the YM field outside the black hole. We also show the energy distribution $E(r)$ of a particlelike solution, where $E(r)$ is the energy of the YM field outside of the radius r . Since the two curves are quite similar, the non-trivial YM structure is almost independent of the existence of the black hole.

l_P/g_C . They may be formed in the early Universe if they are stable. Their quantum effects may be important in that context, so we shall calculate the Hawking temperature of dilatonic colored black holes for various values of α , and discuss their thermodynamical properties. [This includes the known colored black hole as a special case ($\alpha = 0$).] Even if it turns out that those black holes are unstable, it may not diminish their interest. The Hawking temperature, which is simply the surface gravity of the horizon up to a numerical constant, is given as

$$T = \frac{1}{4\pi r_H} e^{-\delta_H} (1 - 2\bar{m}'_H), \quad (13)$$

for the metric (2). The results of plotting $\beta \equiv 1/T$ versus the gravitational mass M are shown in Fig. 5. For the colored black-hole case ($\alpha = 0$), as M increases, T increases within some range of black-hole masses, i.e., for $M_{1,\text{cr}} = 0.905m_P/g_C < M < M_{2,\text{cr}} = 1.061m_P/g_C$ [16]. This means that the specific heat is positive in this mass range. This is hardly surprising, since a colored black hole has similar behavior near the horizon to the Reissner-Nordström black hole. In the case of the Reissner-Nordström black hole, a kind of phase transition occurs, i.e., the specific heat changes its sign as the charge increases beyond some critical charge ($Q_{\text{cr}} \equiv \sqrt{3GM}/2$). The same thing happens here because the effective YM charge of the colored black hole near the horizon increases as M decreases. We find, however, a new behavior: the specific heat changes its sign again if M gets smaller than $0.905 m_P/g_C$. For $M < M_{1,\text{cr}}$, as M decreases β decreases again and vanishes at $M = 0.829m_P/g_C$, when the black hole disappears and a particlelike solution is recovered. To better understand this behavior, we examine the effective charge Q_{eff} of a dilatonic colored black hole (see Fig. 6). For a nondilatonic col-

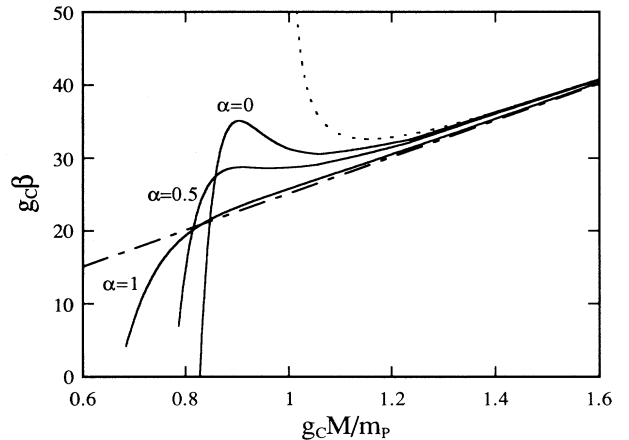


FIG. 5. The inverse temperature $\beta (= 1/T)$ of a dilatonic colored black hole ($n = 1$) for several values of α as a function of M . For $\alpha = 0$ (the colored black hole), the specific heat becomes positive if $0.905m_P/g_C < M < 1.061m_P/g_C$. We find the similar behavior (two phase transitions) for $\alpha < \alpha_{\text{cr}}$ (~ 0.5). For comparison, we also plot the Schwarzschild ($w \equiv 1, \Phi \equiv 0$) and the Reissner-Nordström black-hole cases ($w \equiv 0, \Phi \equiv 0$) by dot-dashed and dotted lines, respectively.

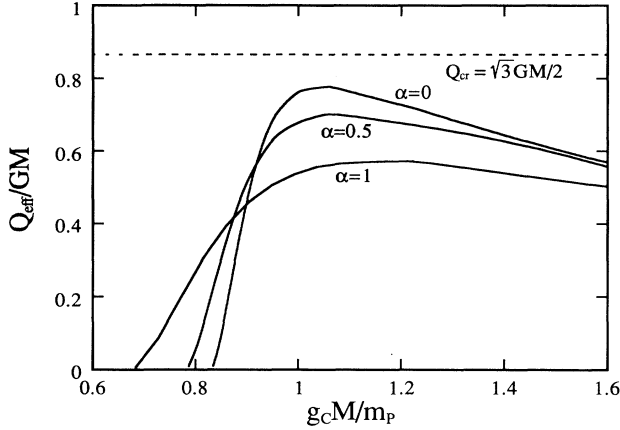


FIG. 6. The effective charge Q_{eff} of the dilatonic colored black hole near the horizon. For $\alpha < \alpha_{\text{cr}} \sim 0.5$, including the colored black hole as a special case ($\alpha = 0$), we find the mass range in which Q_{eff} becomes large and approaches $Q_{\text{cr}} = \sqrt{3}GM/2$.

ored black hole ($\alpha = 0$), Q_{eff}/GM has a maximum at $M = M_{\text{max}} = 1.048m_p/g_C$, when the effective charge is nearly Q_{cr} . M_{max} exists in the interval $[M_{1,\text{cr}}, M_{2,\text{cr}}]$ and Q_{eff}/GM decreases monotonically as the mass departs from M_{max} in both smaller and larger directions. In particular, Q_{eff} vanishes at $M = 0.829m_p/g_C$ where β also vanishes. Hence, the YM field seems to be dominant in the above interval where the specific heat becomes positive. This is the reason why there are two phase transition points for the colored black holes, although the region of large effective charge defined here does not exactly correspond to the mass interval of $[M_{1,\text{cr}}, M_{2,\text{cr}}]$ because of the complicated structure of the black hole and the YM field. At $M = 0.829m_p/g_C$, the event horizon disappears, the temperature is infinite, and the particlelike solution is recovered. Near this mass scale the Hawking black-hole evaporation effect plays an important role in the evolutionary scenario of such a black hole, as we will see later when we discuss the Skyrme black hole.

Similar behavior occurs in the dilatonic colored black hole as well, if the coupling constant α is small enough. This behavior is similar to the EMD black hole, although in the EMD system, there is only one phase transition

point just as in the Reissner-Nordström black hole. From Fig. 4, however, we see that the temperature has a tendency to approach that of the Schwarzschild black hole as α grows, and we find that no phase transition occurs beyond some critical value of α ($\alpha_{\text{cr}} \sim 0.5$). This tendency also makes sense physically, as we can see from Fig. 6, in which we also plot the relation between Q_{eff}/GM and M for various values of α . When α gets larger Q_{eff} becomes smaller. Hence no phase transition occurs.

IV. SKYRME BLACK HOLES

The Skyrme black holes [9] are another type of black holes which have non-Abelian hair. Unlike colored black holes, Skyrme black holes are stable against linear radial perturbations [10]. They may therefore be a legitimate counterexample to the black-hole no hair conjecture. Here we reanalyze the black-hole solutions of the ES system and study their thermodynamical properties in order to compare them with the EYMD system.

The $SU(2) \times SU(2)$ invariant action coupled to gravity is given by [17]

$$S = \int d^4x \sqrt{-g} \left[\frac{1}{2\kappa^2} R(g) + \frac{1}{4} f_S^2 \text{Tr} A^2 - \frac{1}{32g_S^2} \text{Tr} F^2 \right], \quad (14)$$

where F and A are the field strength and its potential, respectively, and f_S and g_S are coupling constants. A and F are expressed in terms of the $SU(2)$ -valued function U as

$$A = U^\dagger \nabla U, \quad F = A \wedge A. \quad (15)$$

Here we are interested in spherically symmetric static solutions, so we make the hedgehog ansatz for U :

$$U(x) = \cos \chi(r) + i \sin \chi(r) \sigma \cdot \hat{r}, \quad (16)$$

where the σ_i denote the Pauli matrices and χ is a function of the radial coordinate r . For the spherically symmetric static spacetime we take the same metric form (2) as in the EYMD case.

Varying the action (14), we obtain the field equations

$$\tilde{m}' = \kappa^2 f_S^2 \left[\frac{\tilde{r}^2}{4} \left(1 - \frac{2\tilde{m}}{\tilde{r}} \right) \chi'^2 + \frac{\sin^2 \chi}{2} + \frac{1}{2\lambda_H^2} \sin^2 \chi \left\{ \left(1 - \frac{2\tilde{m}}{\tilde{r}} \right) \chi'^2 + \frac{\sin^2 \chi}{2\tilde{r}^2} \right\} \right], \quad (17)$$

$$\delta' = -\kappa^2 f_S^2 \left[\frac{\tilde{r} \chi'^2}{2} - \frac{1}{\lambda_H^2} \frac{\chi'^2}{\tilde{r}} \sin^2 \chi \right], \quad (18)$$

$$\left\{ e^{-\delta \tilde{r}^2} \left(1 - \frac{2\tilde{m}}{\tilde{r}} \right) \chi' \right\}' - e^{-\delta} \sin 2\chi + \frac{2}{\lambda_H^2} \sin \chi \left[\left\{ e^{-\delta} \left(1 - \frac{2\tilde{m}}{\tilde{r}} \right) \chi' \sin \chi \right\}' - e^{-\delta} \frac{1}{\tilde{r}^2} \cos \chi \sin^2 \chi \right] = 0, \quad (19)$$

where we have again normalized the scale length by the radius of the event horizon r_H and used the dimensionless variables \tilde{r} and \tilde{m} , as in the EYMD case. $\lambda_H \equiv r_H/[1/f_S g_S]$ describes the ratio of a radius of an event horizon to a typical scale of the present theory.

Note that in the limit $f_S \rightarrow 0$ with $f_S/\lambda_H = g_S r_H$ being finite, the above equations reduce to the colored black-hole case ones when we replace $\cos \chi$ with w and set $g_S^2 = 4\pi g_C^2$ [17].

For the boundary conditions we again demand the ex-

istence of a regular event horizon and asymptotic flatness, that is, we adopt conditions (8), (11) for m and δ . We can restrict the value of χ at the horizon to the range $[-\pi, \pi]$ without loss of generality, because the field equations (17)–(19), or equivalently the action (14), are invariant under the transformation $\chi \rightarrow \chi + 2n\pi$ (n : an integer). Finiteness of the energy of the system gives us the asymptotic boundary condition for χ :

$$\chi(r) \rightarrow 2n\pi \quad \text{as } r \rightarrow \infty, \quad (20)$$

where n is an integer. $|n|$ denotes the winding number of the Skyrme solution. In the case of Skyrme black hole, because its topology is trivial, the winding number, defined by [8]

$$W_n \equiv \frac{1}{2\pi} |\chi(r_H) - \chi(\infty) - \sin[\chi(r_H)]|, \quad (21)$$

is no longer an integer. But, since W_n is close to $|n|$, we also call n the “winding number.”

We solve the field equations (17)–(19) under the above boundary conditions, and find two types of solution. One is a family of solutions which is already discussed in Ref. [10]. It is stable against linear radial perturbations. The other is another family of solutions which has larger gravitational mass M than those of the first family at a given value of the coupling constant and horizon radius. We interpret this as an excited state of the first types of black hole, and as such, it is unstable [8,13]. As discussed in [13], in the limit $f_S \rightarrow 0$, this excited solution approaches a colored black hole of the EYM system, so it is still interesting to study those excited solutions despite their instability.

The stable type of Skyrme black hole has a critical value of $\lambda_{H,\text{cr}}$ for each coupling constant f_S and for each “winding number” n . Beyond this value of λ_H there is no nontrivial solution. For example $\lambda_{H,\text{cr}} = 340.85$ when $f_S/\sqrt{G} = 0.02$, $n = 1$. (See Fig. 7.) This means that a stable Skyrme black hole with large horizon radius (and then with large mass) does not exist. In the previous example, the critical horizon radius and the critical gravitational mass for $g_S = 0.1$ are $r_{H,\text{cr}} = 68.17l_P$ and $M_{\text{cr}} = 46.30m_P$, respectively. The critical value $\lambda_{H,\text{cr}}$ gets small as n increases, i.e., $\lambda_{H,\text{cr}} = 109.19$ for $f_S/\sqrt{G} = 0.02$, $n = 2$ (see also Fig. 7). The family of excited solutions also has a critical value of λ_H , which is the same as that of the stable family. At the critical value $\lambda_{H,\text{cr}}$ two families converge.

This nonexistence of large stable black holes suggests a scenario for the evolution of Skyrme black holes. Suppose we have a stable Skyrme black hole initially. Here we neglect quantum effects, such as black-hole evaporation, on the evolution, although it may be very important as we shall discuss in a moment (Sec. V). When a matter fluid near the event horizon falls into the black hole, the black hole’s mass increases and consequently the radius of its event horizon increases [18,19]. If the horizon radius exceeds the above critical value, the Skyrme black hole shifts to a Schwarzschild black hole. It cannot remain a Skyrme black hole, for no Skyrme black hole has

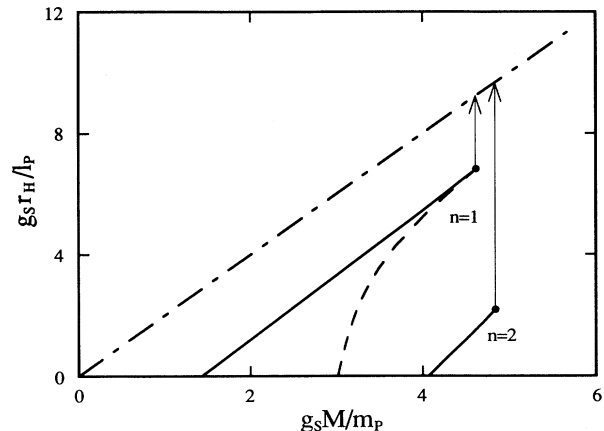


FIG. 7. The relations between mass and horizon radius for the Skyrme black holes. We set $f_S/\sqrt{G} = 0.02$. The dots in the right edges of the lines, where two branches converge, denote the limit of the solutions. Beyond those critical values, there is no Skyrme black hole [8,13]. Hence, by matter accretion, the black hole evolves into a Schwarzschild black hole (a dot-dashed line) as shown by the line with an arrow. In this transition, the area of the black hole changes discontinuously. This may be regarded as a first-order phase transition. For larger “winding number” n , we find larger critical values of the mass while the critical horizon radius becomes smaller.

$M > M_{\text{cr}}$. The Skyrme “hair” may have dropped into the black hole beyond the event horizon, evolving finally into a Schwarzschild black hole. In this sense, a Skyrme black hole may not be stable unless the surroundings are pure vacuum, and in this case the evaporation effect becomes important, as we shall discuss in the next section. One interesting fact is that the area of the Skyrme black hole at the critical mass is smaller than that of the Schwarzschild black hole with the same mass (Fig. 7). Hence when the Skyrme black hole evolves into a Schwarzschild black hole, the area of the black hole jumps sharply, which, because the area can be interpreted as the black-hole entropy, may be regarded as a kind of first-order phase transition.

V. THERMODYNAMICAL PROPERTIES OF SKYRME BLACK HOLES

Since the typical size of a Skyrme black hole ($\sim 1/f_S g_S$) is small, quantum effects such as black-hole evaporation are important. In Fig. 8 we show the temperature of Skyrme black holes. The stable type always has a negative specific heat and has no phase transition like Schwarzschild black holes [Fig. 8(a)]. In case of the excited type, however, the aspect changes drastically [Fig. 8(b)]. For a large coupling constant f_S (e.g., $f_S/\sqrt{G} = 0.03, 0.04$) we find one phase transition point, and black holes with larger mass have positive specific heat. As f_S gets small, the excited Skyrme black hole has three phase transition points: $M_{1,\text{cr}}, M_{2,\text{cr}}, M_{3,\text{cr}}$. The critical point $M_{2,\text{cr}}$ is the same type as that

of the Reissner-Nordström black hole and the smaller one ($M_{1,\text{cr}}$) corresponds to the lower critical point in the colored black-hole type. Between $M_{1,\text{cr}}$ and $M_{2,\text{cr}}$, the specific heat becomes positive, when the Skyrme field becomes dominant. The largest critical point $M_{3,\text{cr}}$ appears only in the Skyrme black hole. Beyond $M_{3,\text{cr}}$, the specific heat becomes again positive. In the limit $f_S \rightarrow 0$, the temperature of a colored black hole is recovered. [Compare the curve of $\alpha = 0$ in Fig. 5 and that of

$f_S/\sqrt{G} = 0.01$ in Fig. 8(b).] This is hardly surprising, because we recover the colored black-hole solution in this limit.

Based on the above properties, we offer the following scenario for the evolution of Skyrme black holes. Because of its instability, we ignore simply the excited type. If its surroundings are simply vacuum, this type of black hole will evaporate away by the Hawking process. The temperature of these black holes, however, becomes infinity when the mass approaches some nonzero finite value, e.g., $M = 14.50m_P$ for $f_S/\sqrt{G} = 0.02$, $g_S = 0.1$. Thus the evaporation process shrinks the event horizon and eventually causes it to disappear; the particlelike solution (Skyrmion) remains. We expect that the Skyrme black hole will evolve into a Skyrmion with a finite mass determined by the fundamental constants (g_S , f_S , and m_P) and the winding number n .

If a matter fluid exists around the black hole, some part of that fluid will fall into the black hole and the black hole's mass will become large, as discussed in Sec. IV. At the same time, the black hole loses mass energy through Hawking process. Which process is more important depends on the mass of the black hole and the density of the surrounding matter fluid. Once the black hole gets large, it shifts to the Schwarzschild one. Therefore we find two simple stories for the Skyrme black holes: (1) The black hole evaporates into the particlelike Skyrmion with a finite mass. It is classically stable. (2) The mass of the black hole increases by matter accretion, it loses its "Skyrme hair," and becomes the Schwarzschild black hole. This will in turn eventually evaporate away, leaving nothing at the end. When the "Skyrme hair" falls into the black hole, the area of black hole increases discontinuously, because the horizon radius becomes larger as the "winding number" vanishes (see the arrows in Fig. 7). Since the area of the black hole is interpreted as the black-hole entropy, we regard this discontinuous jump from the Skyrme black hole to the Schwarzschild black hole as a kind of first-order phase transition.

VI. CONCLUDING REMARKS: DO BLACK HOLES HAVE HAIR, OR DO THEY JUST WEAR WIGS?

We have found black-hole solutions with non-Abelian hair in the Einstein-Yang-Mills-dilaton system, and we have studied their temperatures and specific heats. If the dilaton coupling $\alpha < \alpha_{\text{cr}} \sim 0.5$, these dilatonic colored black holes have two phase transition points, between which the specific heat becomes positive. Although the Skyrme black holes, which also have non-Abelian hair, have no such phase transition point when stable, and their specific heat is always negative, the unstable excited type has some phase transition points like a colored black hole. Because of the absence of Skyrme black holes with large mass, we conclude that such black holes will either evaporate away and leave a stable particlelike non-Abelian structure (Skyrmion) with a finite mass or they will evolve into the Schwarzschild black hole and lose their "Skyrme hair" by matter accretion. This

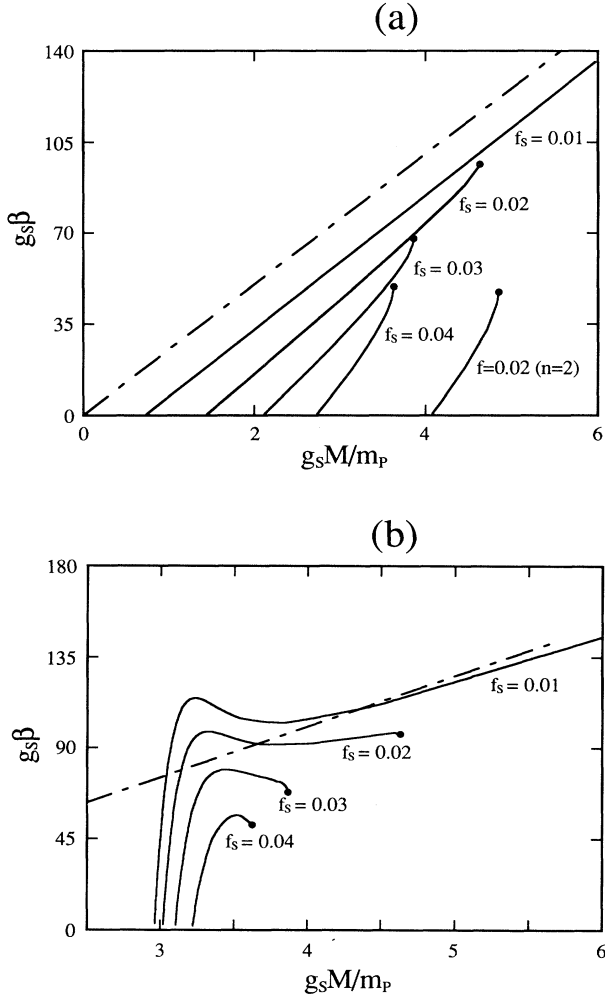


FIG. 8. (a) The inverse temperature β ($= 1/T$) of the Skyrme black hole with $n = 1$ for several values of f_S as a function of M . The dots in the right edges of the lines denote the limit of the solutions, beyond which there is no Skyrme black hole. We also show the inverse temperature of the Schwarzschild black hole by a dot-dashed line for comparison. (b) The inverse temperature $\beta = 1/T$ of the excited types of the Skyrme black holes for several values of f_S as a function of M . The dots in right edges of the solid curves denote the limit of the solutions, which coincide with those of the stable types [see Fig. 8(a)]. As $f_S \rightarrow 0$, the solution approaches the colored black hole. Here we find that it is also true in the behavior of the temperature (compare the curve with $f_S/\sqrt{G} = 0.01$ and $\alpha = 0$ in Fig. 5). The dot-dashed line is that of a Schwarzschild black hole.

Schwarzschild black hole will in turn eventually evaporate away, leaving nothing behind. When the Skyrme black hole evolves into a Schwarzschild black hole, its area (the entropy) will increase by a finite amount, which may be regarded as a kind of first-order phase transition.

As for the stability of dilatonic colored black holes, they may be linearly unstable like “pure” colored black holes. Because the dilaton field Φ has little effect on the potential of the first-order equations for linear perturbations when compared to the colored black-hole case, a bound state (a growing mode) may exist. This is now under investigation.

Although the stability behavior of the colored or dilatonic colored black holes and of the Skyrme black holes is different, we may extract a common property of both sort of non-Abelian “hair” from the present analysis. In the case of the (dilatonic) colored black hole, the YM charge is almost independent of the the black-hole size, as we discussed in Sec. III. When the black hole gets large, it swallows the nontrivial YM structure, thereby acquiring a constant charge. Since the YM field energy from this charge gets small when the black hole gets large, the YM “hair” will contribute little to the black hole’s structure. In the case of the Skyrme black hole, large mass is inconsistent with Skyrme “hair.” Its linear stability may derive from a sort of topological rigidity of non-Abelian gauge fields. Because their “winding numbers” cannot change, linearized perturbations leave them

essentially unaffected. Such a gauge field cannot coexist with a large black hole, however, because they eventually become smaller than the horizon scale. When the black hole gets large, the “Skyrme hair” may disappear behind its horizon. In both cases, the charge or the mass-energy of the non-Abelian gauge field seems to be “quantized” in multiples of the fundamental constants (the Planck mass and the coupling constants) just as for the particle-like solutions. Therefore, when the mass of the black hole gets large, the contribution from these non-Abelian gauge fields becomes small. In the end it vanishes completely, and the trivial Schwarzschild solution results. From these facts, it seems it might be more appropriate to call these non-Abelian structures wigs, instead of hair. A “wig” is independent of the head that wears it (i.e., the black hole), and is more unstable than “hair.” It is easily removed.

ACKNOWLEDGMENTS

We would like to thank T. Maki and T. Tachizawa for discussion and L. D. Gunnarsen for his critical reading of our paper. This work was supported partially by the Grant-in-Aid for Scientific Research Fund of the Ministry of Education, Science and Culture (No. 04234211 and No. 04640312), by a Waseda University Grant for Special Research Projects, and by the Sumitomo Foundation.

-
- [1] P. O. Mazur, *J. Phys. A* **15**, 3173 (1982).
 - [2] J. D. Bekenstein, *Phys. Rev. D* **5**, 1239 (1972).
 - [3] J. B. Hartle, in *Magic without Magic*, edited by J. Klauder (Freeman, San Francisco, 1972).
 - [4] C. Teitelboim, *Phys. Rev. D* **5**, 2941 (1972).
 - [5] R. Bartnik and J. McKinnon, *Phys. Rev. Lett.* **61**, 141 (1988).
 - [6] M. S. Volkov and D. V. Galt’sov, *Yad. Fiz.* **51**, 1171 (1990) [*Sov. J. Nucl. Phys.* **51**, 747 (1990)]; P. Bizon, *Phys. Rev. Lett.* **64**, 2844 (1990); H. P. Künzle and A. K. Masoud-ul-Alam, *J. Math. Phys.* **31**, 928 (1990).
 - [7] N. Straumann and Z.-H. Zhou, *Phys. Lett. B* **243**, 33 (1990); Z.-H. Zhou and N. Straumann, *Nucl. Phys. B* **360**, 180 (1991); P. Bizon, *Phys. Lett. B* **259**, 53 (1991); P. Bizon and R. M. Wald, *ibid.* **267**, 173 (1991).
 - [8] H. C. Luckock and I. Moss, *Phys. Lett. B* **176**, 314 (1986); H. C. Luckock, in *String Theory and Quantum Gravity*, edited by H. J. de Vega and N. Sanchez (World Scientific, Singapore, 1987).
 - [9] S. Droz, M. Heusler, and N. Straumann, *Phys. Lett. B* **268**, 371 (1991).
 - [10] M. Heusler, S. Droz, and N. Straumann, *Phys. Lett. B* **271**, 61 (1991).
 - [11] We learned of the papers by G. Lavrelashvili and D. Maise, *Phys. Lett. B* **295**, 67 (1992), and E. E. Donets and D. V. Gal’tsov, *ibid.* **302** 411 (1993). The former shows the existence of a particlelike solution in the Yang-Mills-dilaton system, while the latter discusses black-hole solutions as well.
 - [12] G. W. Gibbons and K. Maeda, *Nucl. Phys. B* **298**, 741 (1988); for a recent work, see also D. Garfinkle, G. T. Horowitz, and A. Strominger, *Phys. Rev. D* **43**, 3140 (1991).
 - [13] When we were writing this manuscript, we found the paper on the Skyrme black hole by P. Bizon and T. Chmaj, *Phys. Lett. B* **297**, 55 (1992). They have found similar results, e.g., the existence of two types of Skyrme black holes, and the nonexistence of a large black hole, although this was expected from [8]. Although we have not studied linear stability, which they analyzed, we have further discussed the dynamical evolution and the fate of a Skyrme black hole.
 - [14] We use units such that $c = \hbar = k_B = 1$. As for notation and convention we follow C. W. Misner, K. S. Thorne, and J. A. Wheeler, *Gravitation* (Freeman, San Francisco, 1973).
 - [15] H. P. Künzle, *Class. Quantum Grav.* **8**, 2283 (1991); D. V. Galt’sov and M. S. Volkov, *Phys. Lett. B* **274** 173 (1992).
 - [16] The temperature of the colored black hole ($\alpha = 0$) which we calculate disagrees with I. Moss and A. Wray, *Phys. Rev. D* **46**, R1215 (1992). The difference is exactly that from the term $e^{-\delta_H}$ in Eq. (13). They may set $\delta_H = 0$, which is not correct, when they calculate the temperature.
 - [17] We adopt the coupling constant g_S in the ES system, different from g_C in the EYMD system. In order to recover the basic equations in the EYM case in the limit, we have to replace g_S with g_C .
 - [18] D. Sudarsky and R. M. Wald, *Phys. Rev. D* **46**, 1453 (1992).
 - [19] I. Moss, *Phys. Rev. Lett.* **69**, 1852 (1992).